



Diffusional screening in the human pulmonary acinus

M. Felici, M. Filoche and B. Sapoval

J Appl Physiol 94:2010-2016, 2003. doi:10.1152/jappphysiol.00913.2002

You might find this additional information useful...

This article cites 7 articles, 2 of which you can access free at:

<http://jap.physiology.org/cgi/content/full/94/5/2010#BIBL>

Medline items on this article's topics can be found at <http://highwire.stanford.edu/lists/artbytopic.dtl> on the following topics:

- Biochemistry .. Membrane Permeability
- Physiology .. Lungs
- Medicine .. Screening
- Physiology .. Humans

Updated information and services including high-resolution figures, can be found at:

<http://jap.physiology.org/cgi/content/full/94/5/2010>

Additional material and information about *Journal of Applied Physiology* can be found at:

<http://www.the-aps.org/publications/jappl>

This information is current as of December 19, 2006 .

Journal of Applied Physiology publishes original papers that deal with diverse areas of research in applied physiology, especially those papers emphasizing adaptive and integrative mechanisms. It is published 12 times a year (monthly) by the American Physiological Society, 9650 Rockville Pike, Bethesda MD 20814-3991. Copyright © 2005 by the American Physiological Society. ISSN: 8750-7587, ESN: 1522-1601. Visit our website at <http://www.the-aps.org/>.

Diffusional screening in the human pulmonary acinus

M. Felici,¹ M. Filoche,^{1,2} and B. Sapoval^{1,2}

¹Laboratoire de Physique de la Matière Condensée, Centre National de la Recherche Scientifique, Ecole Polytechnique, 91128 Palaiseau; and ²Centre de Mathématiques et leurs Applications, Centre National de la Recherche Scientifique, Ecole Normale Supérieure de Cachan, 94235 Cachan, France

Submitted 3 October 2002; accepted in final form 4 January 2003

Felici, M., M. Filoche, and B. Sapoval. Diffusional screening in the human pulmonary acinus. *J Appl Physiol* 94: 2010–2016, 2003; 10.1152/jappphysiol.00913.2002.—In the mammalian lung acini, O₂ diffuses into quasi-static air toward the alveolar membrane, where the gas exchange with blood takes place. The O₂ flux is then influenced by the O₂ diffusivity, the membrane permeability, and the acinus geometric complexity. This phenomenon has been recently studied in an abstract geometric model of the acinus, the Hilbert acinus (Sapoval B, Filoche M, and Weibel ER, *Proc Natl Acad Sci USA* 99: 10411, 2002). This is extended here to a more realistic geometry originated from the morphological model of Kitaoka et al. (Kitaoka K, Tamura S, and Takaki R, *J Appl Physiol* 88: 2260–2268, 2000). Two-dimensional numerical simulations of the steady-state diffusion equation with mixed boundary conditions are used to quantify the process. The alveolar O₂ concentration, or partial pressure, and the O₂ flux are computed and show that diffusional screening exists at rest. These results confirm that smaller acini are more efficient, as suggested for the Hilbert acini.

oxygen diffusion; acinar gas mixing; mathematical modeling

THE HUMAN PULMONARY acinus, which is the functional unit of gas exchange, has a complicated morphological structure. It comprises the last five to six generations of the bronchial tree, namely the alveolated ducts, originating from one respiratory bronchiole (2, 12). The arrangement in the three-dimensional space of the alveoli is such that the alveolar membrane, where gas exchange takes place, forms a unique, highly irregular surface. O₂ can reach this surface through the alveolated ducts, which form a branched system. It is known that, at this stage, O₂ transport is achieved mainly through diffusion.

In the human lung, at rest conditions, the transition between convective and diffusive transport extends over a zone situated between the first transitional bronchiole and the first generations of the acinus (10). In the diffusion-dominated region, which roughly corresponds to what has been called the 1/8-subacinus by Haefeli-Bleuer and Weibel (2), O₂ diffuses, driven by a partial pressure gradient. This gradient is created by the absorption of O₂ molecules on the alveolar membrane containing the arterious capillaries. The law governing this phenomenon is the well-known Fick's law. The global process includes four main processes

(4): 1) air convective flow; 2) O₂ diffusion in air; 3) diffusion through membrane and plasma; and 4) final binding of O₂ with erythrocytes hemoglobin.

At each of these steps, there is associated a resistance to O₂ transport, depending on the morphology and on the physicochemical transport coefficients. In this work, we study in some detail *step 2*, O₂ diffusion in air, and *step 3*, diffusion through membrane and plasma, and we use an approximate way to take care of convective flow and O₂ binding.

Convection is supposed to become negligible here at the entry of 1/8-subacinus. O₂ transport is then described by the stationary state diffusion into quasi-static air. The rate of binding of O₂ to hemoglobin, which is actually related to the O₂ concentration (or partial pressure) in alveolar air in a nonlinear way through the hemoglobin saturation curve, is here considered to be very large, so that no additional resistance is considered on the blood side. This assumption can be considered as a working hypothesis to be discussed later.

This approach is justified by the recent results that have permitted establishment of a direct link between diffusivity and permeability and the size of the acinus of several mammals from the mouse to the human (10). These last results were obtained through a numerical study of a simplified geometric model of the acinus, called the Hilbert acinus. Our goal here is to study the same type of phenomenon in the more realistic acinus geometry proposed by Kitaoka et al. (3).

The arguments that permit discussion of this question are based on extensive studies carried out on the problem of diffusional transport toward irregular reacting surfaces. This problem is common to a wide class of physical systems and has been addressed in recent years for several cases by means of simple physical models (6, 8). The main concept one has to introduce for a better understanding of such systems is the concept of diffusional screening. Screening means that the particles diffusing toward an irregular absorbing surface are very unlikely to ever reach some deeper regions of the surface because they collide with the nearest and protruding regions of the absorbing surface first. These nearest and protruding regions then act like a "screen" behind which are "hidden" the less

Address for reprint requests and other correspondence: M. Felici, Laboratoire de Physique de la Matière Condensée, CNRS, Ecole Polytechnique, 91128 Palaiseau, France (E-mail: maddalena.felici@polytechnique.fr).

The costs of publication of this article were defrayed in part by the payment of page charges. The article must therefore be hereby marked "advertisement" in accordance with 18 U.S.C. Section 1734 solely to indicate this fact.



accessible regions. The consequence is that only a fraction of the surface is really active, with the relative efficiency (η) of the system being, therefore, diminished. Of course, if the molecules are not absorbed at the first hits on the membrane, they gain a fair chance to explore the deeper regions, which then work and contribute to the overall system efficiency. Because of the serial arrangement of alveoli along the last generations of alveolated ducts, diffusional screening is likely to occur in the pulmonary acinus, which contains 1,000 alveoli. In the following paragraphs, we show that this is the case, at least for rest conditions.

As shown in Refs. 1 and 7, the essential quantity that determines how the system works is a physical parameter, called the “unscreened perimeter length” (Λ). This length, given by the ratio of the O_2 diffusivity to the membrane permeability, is shown to be the unique parameter governing the efficiency of the system for a given geometry.

It is important to notice that screening has the same effect of what has been called in lung physiology “stratified inhomogeneity,” or “stratification” (5), but it is due to a quite different phenomenon. Stratification is related to the idea that the inspired gas has no time to diffuse completely during a normal respiratory cycle so that concentration gradients persist in the lung. On the contrary, diffusional screening characterizes stationary diffusion, that is, the infinite time limit of the diffusion equation. This means that, even after infinite time, the O_2 concentration or partial pressure cannot be completely uniform in the acinus.

THE UNSCREENED PERIMETER LENGTH AND DIFFUSIONAL SCREENING

Let us define the conductance (Y) of the acinus as the flux of O_2 into blood per unit concentration at the entry. For systems in which the final transfer flux is the result of transport in the volume and reaction (here permeation) on the walls, the global Y depends on two contributions: the Y to reach the surface (Y_{reach}) (transport) and the Y to cross the surface (Y_{cross}) (reaction). For the acinus, these two terms depend, respectively, on the diffusion coefficient of O_2 in air ($DO_{2,\text{air}}$) and on the permeability of the alveolar membrane with respect to O_2 (W_{O_2}). The W_{O_2} is defined as the flux across a membrane of unit area per unit concentration difference between the two sides. The relative importance of the two contributions depends also on the shape of the surface, that is, the geometric characteristics of the system. Let us define the diameter of a surface of total area A , length L , as the diameter of the smallest sphere embedding the surface. The diameter represents then the overall size of the system. One can write

$$\begin{aligned} Y_{\text{reach}} &\approx DO_{2,\text{air}}L \\ Y_{\text{cross}} &\approx W_{O_2}A \end{aligned} \quad (1)$$

If one compares Y_{reach} and Y_{cross} , one finds that the condition $Y_{\text{reach}} = Y_{\text{cross}}$ is verified for $DO_{2,\text{air}}/W_{O_2} = A/L$, but the quantity $L_p = A/L$, where L_p is perimeter, is on the order of the mean length of a planar cut of the

surface (11). It is called the perimeter of the surface. Obviously, the L_p depends on its shape. If the surface is a sphere, its area is $A \propto L^2$ and then $L_p = A/L \propto L$, which is of order L . On the contrary, if the surface is very irregular, it may exhibit $L_p = A/L \gg L$.

Therefore, the condition $Y_{\text{reach}} = Y_{\text{cross}}$ amounts to $A/L = DO_{2,\text{air}}/W_{O_2} = \Lambda$, where Λ is the ratio of the diffusion coefficient by the permeability. The last condition then reads $L_p = \Lambda$. Although Λ is a length given by the physical parameters of the system, L_p depends uniquely on the morphology, shape, and size of the surface.

It is now possible to better understand the concept of screening. Screening occurs when a portion of the surface is not reached. This happens if $Y_{\text{reach}} < Y_{\text{cross}}$ ($\Lambda < L_p$). In this case, the Y of the system is limited by the Y to reach the surface. On the contrary, if $Y_{\text{reach}} > Y_{\text{cross}}$ ($\Lambda > L_p$), the surface works uniformly, and the total Y is limited by the Y to cross the surface.

If one considers a region of the surface with a perimeter smaller than Λ , for that region $Y_{\text{reach}} \geq Y_{\text{cross}}$. This region then works uniformly, and screening is not effective. This is the reason why Λ is called unscreened perimeter length. On the contrary, a region with a perimeter greater than Λ does not work in a uniform way. In a different language, the length Λ measures, through its perimeter, the size of the region of the exchange surface that a molecule of O_2 explores, on average, before being absorbed.

This applies to irregular surfaces that present no deep pores (9). Consider, for example, a pore of length L and diameter d , for which $L_p = 2L$. It has an access Y of order Dd^2/L and a surface Y of $W\pi dL$. They are equal if $\Lambda = \pi L^2/d = L_p \cdot (\pi L/2d)$. If Λ is smaller than this last length, there is screening, and the pore walls do not work uniformly. Then screening depends both on the “perimeter” L_p of the pore and the quantity $(\pi L/2d)$, which is the pore aspect ratio (always >1). With the acinus being a deeply porous structure, one expects that screening will depend both on the acinus perimeter and on a factor (always >1) related to the porous nature of the geometry.

Screening phenomenon has so far been neglected in the study of gas mixing in the pulmonary acinus, although the idea was qualitatively described in Weibel’s book (12). This problem has been precisely formulated from a physical point of view in Refs. 7–10.

THE MATHEMATICAL MODEL

The acinus is a compact bounded structure. There is one inlet, from which fresh air enters the structure. The empty space in the ducts is bounded by a connected gas exchange surface with an average total area of 8.63 cm^2 (2). These data refer to the $1/8$ -subacinus, which is usually considered as the actual gas-exchange unit for the human lung.

In the steady-state condition, the space-dependent concentration $C(x, y, z)$ of O_2 in air obeys the Laplace equation

$$\frac{\partial^2 C}{\partial x^2} + \frac{\partial^2 C}{\partial y^2} + \frac{\partial^2 C}{\partial z^2} = 0 \tag{2}$$

We have chosen here to write all of the equations in terms of the alveolar O₂ concentration C; one might consider equivalently the same equations for the partial pressure of O₂ in alveolar air. According to Fick's law, the O₂ current *J* is given by

$$\vec{J} = -D_{O_2,air} \vec{\nabla} C \tag{3}$$

The net current across the membrane is given by

$$J_n = W_{O_2} C \tag{4}$$

where *J_n* is the normal component of the current entering the surface. In this simplified frame, blood is considered to work as an O₂ sink, and thus the concentration of O₂ in it is put equal to zero. Then *C*(*x*, *y*, *z*) in Eq. 4 is the concentration of O₂ in alveolar air at the interface with the membrane.

The boundary conditions at the surface can be obtained by imposing the conservation of current across the membrane $-D_{O_2,air} \partial C / \partial n = W_{O_2} C$, where *n* refers to the direction normal to the interface. As a boundary condition for the entry of the acinus, we consider a fixed concentration *C*₀. This means that the source of diffusion, i.e., the diffusion front, is supposed to sit at the entrance of the subacinus. We then neglect convection from there on. The concentration of O₂ in the acinus is described by the following set of equations

$$\begin{cases} \frac{\partial^2 C}{\partial x^2} + \frac{\partial^2 C}{\partial y^2} + \frac{\partial^2 C}{\partial z^2} = 0 & \text{in the bulk} \\ C = C_0 & \text{at the source of diffusion} \\ \frac{\partial C}{\partial n} = -\frac{1}{\Lambda} C & \text{at blood-air interface} \end{cases} \tag{5}$$

These equations imply the assumption of stationarity, which can be considered valid during inspiration at normal (rest) breathing. The physical parameters in the problem are *D*_{O₂,air} and *W*_{O₂}, although they appear only in the form of their ratio Λ .

The value of *D*_{O₂,air} = 0.178 cm²/s (12). The value of the permeability depends on the solubility of O₂ in

physiological tissue, considered to be water, and the diffusion barrier between air and the erythrocytes (including the thickness of the membrane and the thickness of the plasma layer). Taking the values from literature (13), it is found that $\Lambda \approx 30$ cm.

The Geometric Model

This mathematical model, illustrated in Eq. 5, is applied to the geometric model of the pulmonary acinus recently proposed by Kitaoka et al. (3). The acinar structure is simulated by using a labyrinthine algorithm. The 1/8-subacinus is approximated to be a set of cubic cells with a side dimension of 0.5 mm; alveoli are generated by attaching alveolar septa 0.25 mm long and 0.1 mm wide to the inner walls of each such cell. The algorithm is designed to construct a three-dimensional branching tree without loops that starts from one entrance and passes through all cells, filling completely the given space. Random variables enter in the construction of the intra-acinar pathways so that it is possible to obtain different structures within the same global size, having the same mean path length and the same total area. The values of mean path length, surface area, and numbers of ducts and sacs are chosen to fit the morphological data reported in the literature (2). A two-dimensional (2D) realization of such a geometry is shown in Fig. 1.

NUMERICAL SIMULATIONS

Equation 5 has been solved in 2D in the Kitaoka 2D geometry by means of finite-element computations by using MATLAB PDE Toolbox. Different values of Λ have been considered, as well as acini with several sizes.

The computation has been carried on for the two types of geometry shown in Fig. 1: first, with *type A* geometry in which alveolar septa are present on the ducts walls (Fig. 1A), and second, on a simplified *type B* geometry in which the septa are missing (Fig. 1B). As shown below, the presence of the septa does not affect the overall behavior of the system, if one properly rescales the unit length. Therefore, most of the compu-

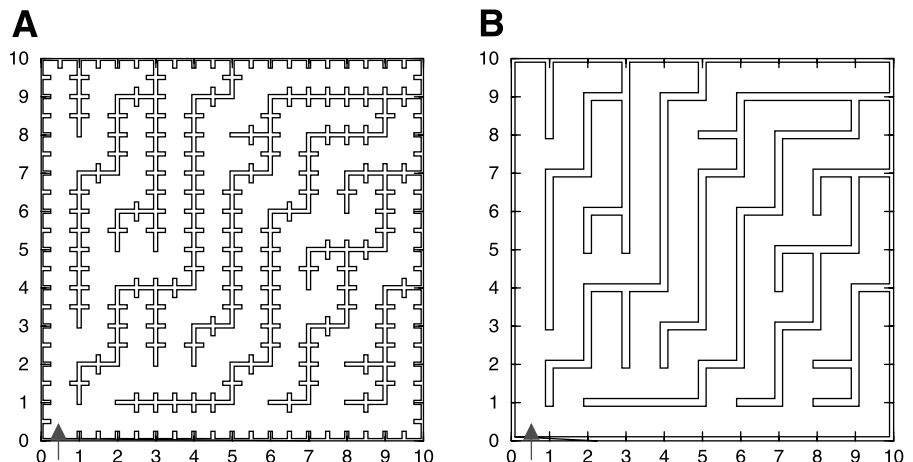


Fig. 1. Example of a two-dimensional realization of an acinus of size 10 × 10 obtained from the labyrinthine algorithm of Kitaoka et al. (3) (the side of the square cells is taken as the unit length). The entry is located at the bottom left, cell 0,0. The mean path length is 12.93, which corresponds to 6.465 mm. A: alveolar septa are present, total perimeter (i.e., total alveolar “surface”) is *L_p* = 320.4 or 160.2 mm. B: the same geometry without alveolar septa, *L_p* = 200 or 100 mm.

tations have then been performed on the simplified *type B* geometry.

The result for one acinus of size 20×20 (400 cells) is shown in Fig. 2, in which the O_2 concentration distribution is imaged for four values of Λ . It can be seen qualitatively that, for values of Λ smaller than the perimeter, only a fraction of the surface actually works (red regions in Fig. 2).

To characterize in a quantitative manner the effect of screening, we introduce the acinus efficiency (η), which measures the fraction of the surface that is really active. The η is defined as the ratio of the total flux Φ across the absorbing membrane to the flux in ideal conditions (infinite diffusivity or infinite Λ). The inlet flux is given by

$$\Phi = \int_{\text{entry}} D_{O_2, \text{air}} \partial C / \partial n \, dl \quad (6)$$

where the integral is over the section of the entrance duct, and l is the coordinate along the interface (curvilinear coordinate). Because of the flux conservation, it is also equal to the total outlet flux

$$\Phi = \int_{L_p} W_{O_2} C \, dl \quad (7)$$

where the integral is computed over the whole absorbing perimeter.

The ideal flux Φ_{id} is the total flux that one would have if the O_2 had perfectly spread in the volume. In

that case, the concentration is equal to C_0 everywhere in the system and

$$\Phi_{id} = W_{O_2} C_0 L_p \quad (8)$$

The Φ_{id} is then the flux for a system working in a perfectly uniform way. The efficiency is a number between 0 and 1 that measures the relative fraction of active surface.

It should be emphasized that larger efficiency does not imply larger flux. An “efficient” acinus is “better used” in the sense that the whole acinar surface is working for transfer. The introduction of the efficiency concept is necessitated by the fact that the overall functioning of the acinus depends on three independent parameters: the diffusivity, the permeability, and the geometry. As shown below, the problem can be simply understood in terms of only two parameters, the length Λ and the geometry. The flux itself increases with $D_{O_2, \text{air}}$, with everything else constant, and with W_{O_2} , with everything else constant. The dependence of the flux on the system size for constant $D_{O_2, \text{air}}$ and W_{O_2} is related to the efficiency. The flux can be written as

$$\Phi = W_{O_2} C_0 \cdot \eta L_p \quad (9)$$

One can compute numerically η and study its behavior as a function of the acinus size and the Λ . The results are shown in Fig. 3. The efficiency increases with a power law for values of $\Lambda \leq L_p$. For larger values of Λ , it approaches 1. The power law exponent is found to be around $\alpha = 0.74$, independent of the acinar size. If one compares the curves $\eta(\Lambda)$ obtained for the geometries of Kitaoka et al. (3) with those presented in Ref.

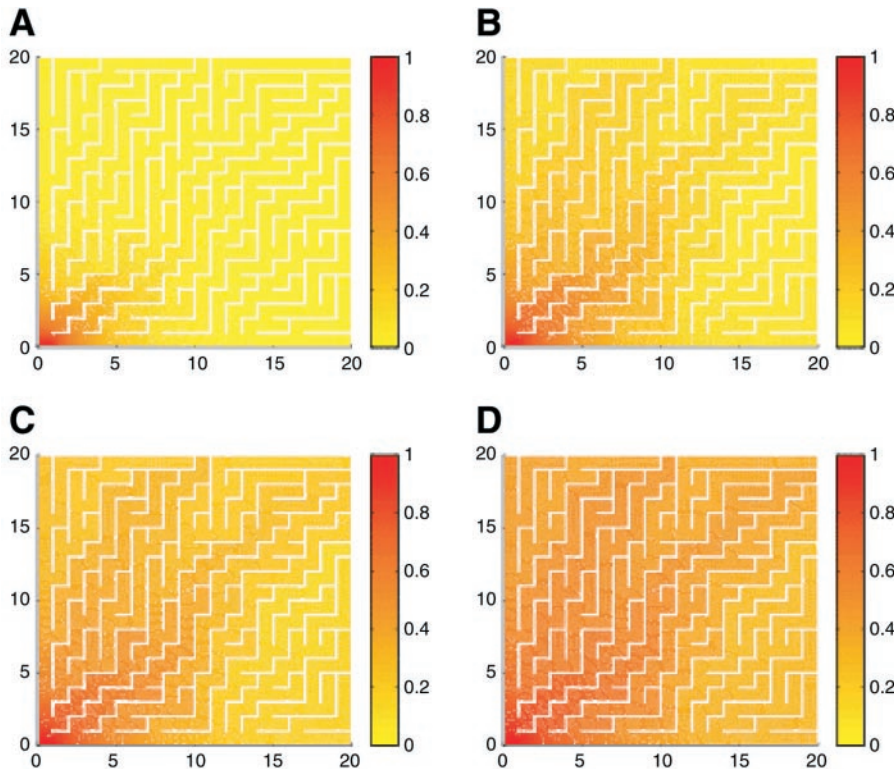


Fig. 2. O_2 concentration or partial pressure field for four values of the unscreened perimeter length $\Lambda = 80$ (A), $\Lambda = 500$ (B), $\Lambda = 1,000$ (C), and $\Lambda = 2,000$ (D).

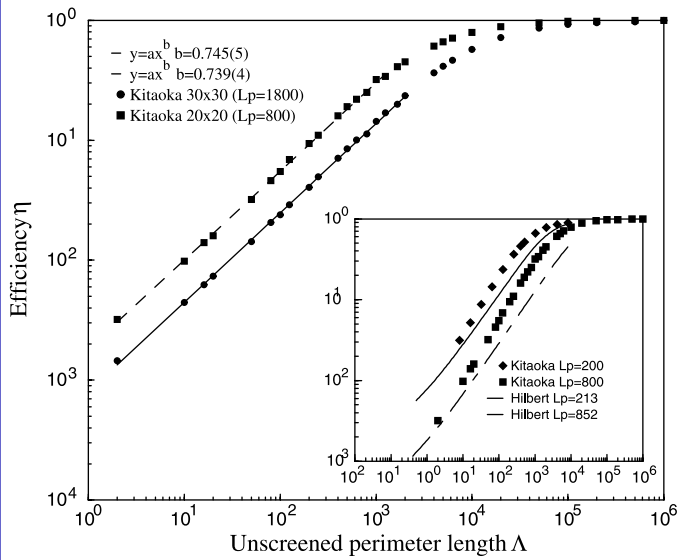


Fig. 3. Acinar efficiency η as a function of Λ . The power law fit $\eta = \Lambda^\alpha$ for the first part of the graph gives $\alpha = 0.745 \pm 0.005$ for the acinus of size 30 and $\alpha = 0.739 \pm 0.004$ for the acinus of size 20. In human lungs, $\Lambda = 600$. *Inset*: η as a function of Λ for Kitaoka (3) geometries (\blacklozenge , $L_p = 200$; \blacksquare , $L_p = 800$) and Hilbert geometries (10) (solid line, $L_p = 213$; dashed line, $L_p = 853$).

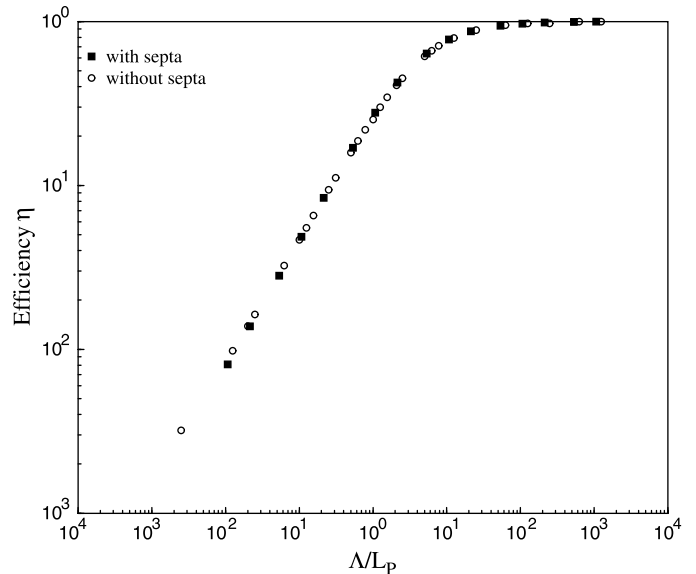


Fig. 4. The η for models with and without alveolar septa. If the efficiency is given against Λ/L_p , the 2 curves collapse into the same curve. This collapse indicates that the details of the morphology do not play any significant role in the global η .

10 for the Hilbert geometry, one can observe that the general trend is the same, but there are significant qualitative and quantitative differences (see Fig. 3, *inset*). The power law exponent for the first part of the curve is different in the two cases. One can conclude that the response of the system depends on its geometric structure, or branching pattern. Comparing the results for a Kitaoka geometry and a Hilbert geometry, it is found that efficiency is larger for the more realistic Kitaoka acinus. This is due mainly to a peculiarity of the Hilbert construction, which presents a bottleneck near the entry.

In Fig. 4, the efficiencies resulting from the computation in the two types of geometries, with and without septa, are compared: the behavior of η with Λ varying is exactly the same if one rescales Λ with the perimeter, which has different values in the two cases. This means that not only the behavior of the physical quantities in *type A* geometry can be inferred from the computations on geometry of *type B* but also the quantitative results for *type A* can be obtained from those of *type B* through a simple rescaling. This insensitivity to geometric details is a general property of diffusional processes, due to the smoothing character of the Laplace operator (1). Moreover, this indicates that the proper parameter governing the system is indeed the ratio of the Λ to the total perimeter.

The total number of alveoli in one $1/8$ -subacinus is $\sim 1,000$. In the 2D Kitaoka model, each square cell comprises four alveoli (two on each side), and the alveolus size is 0.25 mm, corresponding to $(1/2)\ell$, where ℓ is the square cell size (we put $\ell = 1$). In our units, the size of a square containing 1,000 alveoli is then $L \approx 20$ while $\Lambda \approx 600$. As the perimeter of the 20×20 acinus is $L_p = 800$, we are in the regime $\Lambda \leq L_p$, where

screening is effective. For these values, the efficiency is found to be on the order of 25%. As these are the realistic conditions for a human subacinus at rest, this result indicates that screening is effective and reduces significantly the lung efficiency in rest conditions.

If one considers the efficiency as a function of the size, smaller acini are found to be more efficient. This is shown in Fig. 5, which gives the dependence of η on size. In fact, for a given Λ , the absolute size of the active region is approximately constant, and an increase of the total perimeter length only has the effect of diminishing the fraction of effective surface and thus

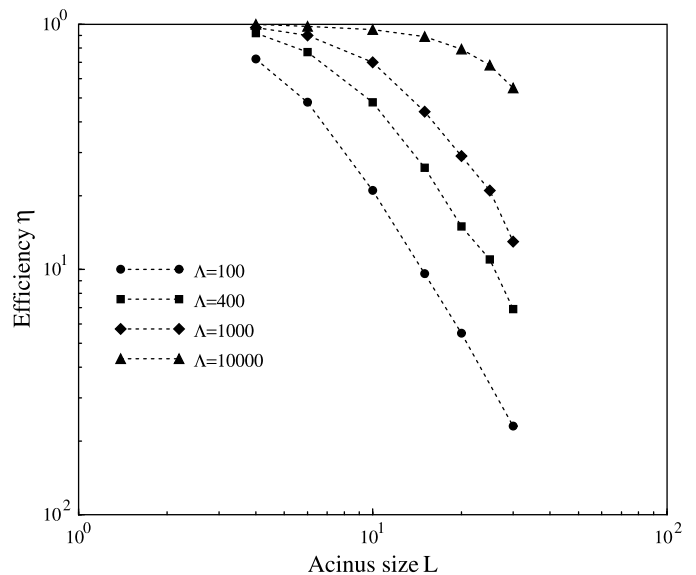


Fig. 5. Efficiency η as a function of the acinus size. The 4 curves refer to different values of Λ . The efficiency decreases with size as soon as the perimeter becomes comparable with Λ . The size of a human acinus corresponds roughly to length $L = 20$.

the efficiency. Therefore, optimization of diffusional transport requires small acini. This result is general and would be obtained whatever the details of the acinus morphology were. On the other hand, as the effectiveness of convective flow is limited by the diameter of the ducts (hydrodynamic resistance growing as the fourth power of the inverse diameter), the conducting ducts should not be too narrow. These considerations suggest that the actual size of the acini might be the result of a compromise between these two requirements.

DISCUSSION

In this frame, the acinus is only partly efficient at rest. However, it is known that, at exercise, the total uptake of O_2 can be increased by a factor of 10. It is generally admitted that the pulmonary system is working with maximal efficiency at exercise. Along the above lines, the reason for it is that the transition between convective flow and diffusional transport occurs deeper in the acinus at exercise, due to the increase of the inlet velocity of air (10). This means that, in our model, at exercise, the source of diffusion, where the concentration is fixed at C_0 , should be put inside the acinus. The regions that are not active at rest then become accessible to diffusing O_2 , and the global efficiency may rise up to 100%. This “uncovering” or “unscreening” of portions of alveolar surface nonactive at rest might then be one of the reasons explaining the rise in the metabolic rate from rest to exercise.

It may be useful to discuss briefly the concept of stratification, which is a subject of much controversy. We define stratification here as the presence of concentration gradients during the inspiration transitory regime. As a matter of fact, with diffusion speed being finite, for small periods of time, O_2 cannot reach the regions that are “too far.” In this sense, stratification can be seen as being really the dynamic screening. Inspiration covers a time t_I , and O_2 needs a time $t_t < t_I$, where t_t is the time to reach the stationary state from the beginning of inspiration. Before time t_t , O_2 profile evolves in time, penetrating more and more into the acinus; therefore, O_2 concentration is not homogeneous in the structure because of stratification. After reaching the stationary state, O_2 profile does not change any more, but concentration gradients are present because of diffusional screening, as it has been shown above. Given the diffusion coefficient of O_2 and the linear dimensions of the acinus, t_t can be evaluated to be on the order of 1 s. This means that 1) the transitory regime is not totally negligible in the respiratory cycle, and 2) concentration gradients persist even in the stationary state. O_2 concentration is then never homogeneous within the acinus.

Note that the fact that the computation was done in a 2D structure should not be considered as a serious defect of the results, because the real acinus is a tree structure. The diffusion paths must then follow the tree branches, whatever the dimensionality. In that case, the behavior of the system depends directly on its

topology. This is why it is important to consider a geometric model that reproduces the topological features of the real system.

The model presented here addresses the problem of gas mixing for the whole acinus to investigate the effect of the morphological characteristics on its functioning. This model focuses on the diffusional transport mechanism and deals with the other phenomena, as convective flow and binding dynamics, in an approximated way. In this approach, the binding rate of O_2 by hemoglobin has been supposed to be large enough so that it does not limit the net O_2 transfer.

In exercise conditions, when the increase in airflow velocity allows convection to push the diffusion source inside the acinus, as discussed above, screening should be negligible. The O_2 partial pressure should then be uniform, and an average value for O_2 binding could be used. Conversely, the average O_2 binding could be deduced from the comparison between physiology and geometry.

The results show evidence that the acinus is not at maximal efficiency at rest because of screening. The effect is far from being negligible, with the computed efficiency being on the order of 25%. The size of the acinus is shown on general grounds to be limited by the existence of a finite Λ . Our results generalize those recently obtained in the artificial picture of the so-called Hilbert acinus (10) to the more realistic Kitaoka models of the human pulmonary acinus (3).

In particular, it is interesting to notice that, as a consequence of screening, small animals should be more efficient than big ones, which have larger acini. It is indeed a well-known fact that the O_2 uptake per unit body mass decreases with animal mass, as known from the allometric law of the metabolic rates.

Further studies of the O_2 flux at rest should include a nonlinear binding function of O_2 concentration, related to the hemoglobin saturation curve. The main limitations of this model appear in that convection is neglected, with the transition from convection to diffusion being modeled here as being sharp. Because of the stationarity assumption, the changes in the acinar volume occurring during the respiratory cycle are not accounted for as well. Further studies on more detailed models, including nonlinear O_2 binding, should investigate the interplay between the different phenomena.

The Centre de Mathématiques et de leurs Applications and the Laboratoire de Physique de la Matière Condensée are Unité Mixte de Recherches du Centre National de la Recherche Scientifique nos. 8536 and 7643, respectively.

REFERENCES

1. **Filoché M and Sapoval B.** Transfer across random versus deterministic fractal interfaces. *Phys Rev Lett* 84: 5776–5779, 2000.
2. **Haefeli-Bleuer B and Weibel ER.** Morphometry of the human pulmonary acinus. *Anat Rec* 220: 401–414, 1988.
3. **Kitaoka K, Tamura S, and Takaki R.** A three-dimensional model of the human pulmonary acinus. *J Appl Physiol* 88: 2260–2268, 2000.

4. **Paiva M and Engel LA.** Model analysis of intra-acinar gas exchange. *Respir Physiol* 62: 257–272, 1985.
5. **Paiva M and Engel LA.** Theoretical studies of gas mixing and ventilation distribution in the lung. *Physiol Rev* 67: 750–796, 1987.
6. **Rosso M, Huttel Y, Chassaing E, Sapoval B, and Gutfraind R.** Visualization of an irregular electrode by optical absorption. *J Electrochem Soc* 144: 1713–1717, 1997.
7. **Sapoval B.** Transfer to and across irregular membranes modeled by fractal geometry. In: *Fractals in Biology and Medicine*, edited by Nonnenmacher TF, Losa GA, and Weibel ER. Basel: Birkhäuser, 1994, p. 241–249.
8. **Sapoval B.** Transport across irregular surfaces: fractal electrodes, membranes and catalysts. In: *Fractals and Disordered Systems* (2nd ed.), edited by Bunde A and Havlin S. Berlin: Springer-Verlag, 1996.
9. **Sapoval B, Filoche M, Karamanos K, and Brizzi R.** Can one hear the shape of an electrode? I. Numerical study of the active zone in Laplacian transfer. *Eur Phys J B* 9: 739–753, 1999.
10. **Sapoval B, Filoche M, and Weibel ER.** Smaller is better—but not too small: a physical scale for the design of the mammalian pulmonary acinus (Abstract). *Proc Natl Acad Sci USA* 99: 10411, 2002.
11. **Weibel ER.** *Stereological Methods*. London: Academic, 1980, vol. 2.
12. **Weibel ER.** *The Pathway for Oxygen*. Cambridge, MA: Harvard University Press, 1984.
13. **Weibel ER, Federspiel WJ, Fryder-Doffey F, Hsia CCW, Konig M, Stadler-Navarro V, and Vock R.** Morphometric model for pulmonary diffusing capacity. I. Membrane diffusing capacity. *Respir Physiol* 93: 125–149, 1993.

